Photoalignment of a Nematic Liquid Crystal Fluid and Glassy−Nematic Oligofluorenes on Coumarin-Containing Polymer Films

Anita Trajkovska,[†] Chunki Kim,[†] Kenneth L. Marshall,[‡] Thomas H. Mourey,[§] and Shaw H. Chen*[,†,‡]

Department of Chemical Engineering and Laboratory for Laser Energetics, University of Rochester, 240 East River Road, Rochester, New York 14623-1212, and Foundation Science Center, Eastman Kodak Co., 1999 Lake Avenue, Rochester, New York 14650-2106

Received April 30, 2006; Revised Manuscript Received July 25, 2006

ABSTRACT: The orientations of both a nematic liquid crystal fluid and a series of monodisperse glassy−nematic oligofluorenes were investigated on photoalignment films comprising a polymethacrylate backbone with 7-benzoyloxycoumarin pendants. Both classes of liquid crystalline material were found to undergo a transition from a parallel to a perpendicular orientation with reference to the polarization axis of UV-irradiation at a sufficiently high extent of dimerization. The UV−vis and FTIR spectroscopic analyses revealed photostability with irradiation up to a fluence of 10 J/cm^2, thereby excluding photodegradation as the basis for the observed crossover. A kinetic model was used to interpret the crossover behavior for irradiation at 25 °C, leading to the conclusion that liquid crystal molecules interact more favorably with coumarin monomers than with dimers. Through thermal annealing above T_g followed by cooling to room temperature, a glassy−nematic pentafluorene film was prepared on a photoalignment film, exhibiting an orientational order parameter comparable to that on a rubbed polyimide film. At an increasing oligofluorene chain length, however, a decreasing orientational order parameter emerged, presumably because of the increased annealing temperature that causes an orientational relaxation on the part of the dimerized coumarin moieties.

Introduction

Mechanical rubbing is a traditional approach to accomplishing uniaxial orientation of liquid crystal fluids in electro-optic devices. More recently, rubbing has also been demonstrated to be capable of orienting π-conjugated oligomers and polymers for the fabrication of polarized light-emitting diodes[1−6] and field-effect transistors.[7−10] However, the inevitable electrostatic charges and dust particles as well as the potential physical damage to the rubbed alignment film are known to adversely affect device performance and lifetime.[11,12] To circumvent these problems, photoalignment has been actively explored as a noncontact method, which also enables patterning for the realization of wide viewing angles in liquid crystal displays[13] and tunability in electro-optic devices.[14−16] There are three distinct material approaches to photoalignment: anisotropic degradation of polyimides,[17−21] *cis-trans* isomerization of azobenzenes,[22−28] and anisotropic (2 + 2) cycloaddition of cinnamates[29−37] or coumarins.[13,37−42] Some of these photoalignment techniques have been implemented in liquid crystal displays,[13,43] polarized light-emitting diodes,[44−46] and field-effect transistors.[47,48] Because of thermal and photochemical stability without complication from photoinduced isomerization, we have aimed at coumarin-containing polymethacrylates for an elucidation of the transition of liquid crystal orientation from a parallel to a perpendicular orientation at a critical fluence, i.e. the intensity of polarized UV-irradiation. In a recent paper,[49] we have quantified the extent of photodimerization as the ultimate parameter controlling the crossover behavior of photoalignment films comprising polymethacrylates with 6- and 7-substituted coumarin pendants. Moreover, we have constructed a kinetic model to evaluate the relative importance of three factors: the relative abundance of coumarin dimers and monomers, the evolution of their orientational order, and the energetics of molecular interaction. It is encouraging to note that the photoalignment films are capable of orienting a nematic liquid crystal to an order parameter between 0.70 and 0.78, comparable to that attainable with rubbed polyimide films. Inspired by recent reports on the ability of a UV-irradiated film of **Polymer** (poly-[7-[[4-[[[6-(methacryloyl)oxy]hexyl]oxy]benzoyl]oxy]coumarin]), as depicted in Chart 1, doped with a hole conductor[44] to orient reactive π-conjugated mesogens, the present work was undertaken to furnish fundamental insight into liquid crystal orientation, including the possible role of photodegradation,[39] and to test the feasibility of generating well ordered glassy−nematic films of monodisperse oligofluorenes[4−6,10] for potential use in organic electronics devices.

Experimental Section

Materials Synthesis. The reaction schemes as well as the synthesis and purification procedures for **Polymer**, **Copolymer**, **Monomer**, and **Dimer** are included in Supporting Information. The analytical and ^{1}H NMR spectral data are presented in what follows.

Poly[7-[[4-[[[6-(methacryloyl)oxy]hexyl]oxy]benzoyl]oxy]-coumarin], Polymer. Anal. Calcd: C, 69.32; H, 5.82. Found: C, 68.82; H, 5.88. ^{1}H NMR spectral data (400 MHz, $CDCl_3$): δ (ppm) 0.90−1.83 (13H, polymer main chain and spacer linkage), 3.99 (4H, −COOCH_2−, −CH_2OAr−), 6.35 (1H, −HC═C*H*CO−, coumarin), 6.91 (2H, aromatics), 7.13 (2H, coumarin), 7.50 (1H, coumarin), 7.69 (1H, −*H*C═CHCO−, coumarin), 8.05 (2H, aromatics).

Poly[MMA-*co*-[7-[[4-[[[6-(methacryloyl)oxy]hexyl]oxy]benzoyl]-oxy]coumarin]], Copolymer. Anal. Calcd: C, 66.23; H, 6.51.

* To whom correspondence should be addressed. E-mail: shch@lle.rochester.edu.
† Department of Chemical Engineering, University of Rochester.
‡ Laboratory for Laser Energetics, University of Rochester.
§ Eastman Kodak Co.

10.1021/ma060959s CCC: $33.50
Published on Web 09/06/2006

Chart 1. Polymer, Copolymer, Monomer, and Dimer Synthesized for This Study[a]

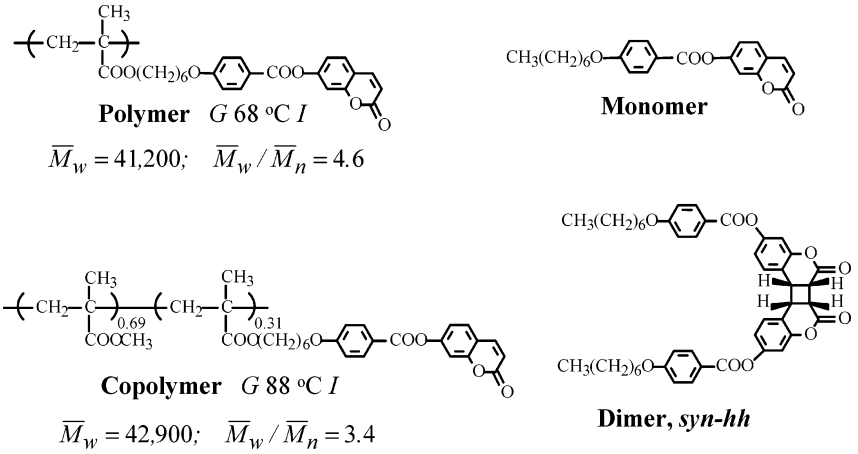

[a] Symbols: G, glassy; I, isotropic; $\bar{M}_w$ and $\bar{M}_n$, weight- and number-average molecular weights, Respectively. Regioisomerism identified as *syn-hh* in the Supporting Information.

Found: C, 65.66; H, 6.66. ^{1}H NMR spectral data (400 MHz, $CDCl_3$): δ (ppm) 0.90−1.83 (polymer main chain and spacer linkage), 3.58 (−COO*CH*$_3$) 3.99 (−C*H*$_2$OAr−), 4.04 (−COOC*H*$_2$−), 6.38 (−HC═C*H*CO−, coumarin), 6.96 (aromatics), 7.18 (coumarin), 7.51 (coumarin), 7.70 (−*H*C═CHCO−, coumarin), 8.10 (aromatics).

7-[[4-(Heptyloxy)benzoyl]oxy]coumarin, Monomer. Anal. Calcd: C, 72.61; H, 6.36. Found: C, 72.81; H, 6.37. ^{1}H NMR spectral data (400 MHz, $CDCl_3$): δ (ppm) 0.89 (t, 3H, *CH*$_3$CH$_2$), 1.29−1.40 (m, 6H, CH$_3$*CH*$_2$CH$_2$CH$_2$CH$_2$), 1.48 (q, 2H, −*CH*$_2$CH$_2$CH$_2$-OAr−), 1.82 (q, 2H, −C*H*$_2$CH$_2$OAr−), 4.05 (t, 2H, −C*H*$_2$OAr−), 6.40 (d, 1H, −HC═C*H*CO−, coumarin), 6.97 (d, 2H, aromatics), 7.17 (d, 1H, coumarin), 7.23 (s, 1H, coumarin), 7.52 (d, 1H, coumarin), 7.71 (d, 1H, −*H*C═CHCO− coumarin), 8.12 (d, 2H, aromatics).

(6aα,6bα,12bα,12cα)-6a,6b,12b,12c-Tetrahydro-3,10-bis[[4-(heptyloxy)benzoyl]oxy]cyclobuta[1,2-c:4,3-c′]dicoumarin, Dimer. Anal. Calcd: C, 72.61; H, 6.36. Found: C, 72.34; H, 6.23. ^{1}H NMR spectral data (400 MHz, $CDCl_3$): δ (ppm) 0.89 (t, 6H, *CH*$_3$CH$_2$), 1.30−1.39 (m, 12H, CH$_3$*CH*$_2$CH$_2$CH$_2$CH$_2$), 1.46 (q, 4H, −*CH*$_2$-CH$_2$CH$_2$OAr−), 1.81 (q, 4H, C*H*$_2$CH$_2$OAr), 4.02 (t, 4H, −C*H*$_2$-OAr−), 4.08 (m, 2H, cyclobutane), 4.22 (m, 2H, cyclobutane), 6.81−6.99 (m, 10H, coumarin and aromatics), 8.08 (d, 4H, aromatics).

Transition Temperatures and Polymer Molecular Weights. Thermal transition temperatures of **Polymer** and **Copolymer** were determined by differential scanning calorimetry (DSC Perkin-Elmer DSC-7) with a continuous N_2 purge at 20 mL/min. Samples were preheated to 200 °C followed by cooling to −30 °C before taking the reported heating and cooling scans at 20 °C/min. The nature of phase transitions was characterized with a polarizing optical microscope (DMLM, Leica, FP90 central processor) coupled with a hot stage (FP82, Mettler Toledo). Their molecular weights were determined by a size-exclusion chromatograph (Model 2695 separations module, a 2487 spectrophotometric detector, and a 410 differential refractive index detector, all from Waters Corp., Milford, MA, and a model 110 differential viscometry detector, Viscotek, Porter, TX) in *N*,*N*-dimethylformamide containing 0.01 M lithium nitrate at 35 °C on the basis of a universal calibration curve established with poly(methyl methacrylate) standards (Polymer Laboratories, Church Stretton, UK).

Film Preparation and Characterization. Photoalignment films were prepared with **Polymer** by spin casting at 4000 rpm from 0.1 wt % chloroform solutions on optically flat fused silica substrates transparent to 200 nm (EscoProducts). For UV−vis (Hewlett-Packard 8453E) and FTIR (Brüker IFS/66 spectrometer) measurements, approximately 10- and 25-nm-thick films were spin-cast at 4000 rpm from 0.1 and 0.3 wt % chloroform solutions, respectively, on calcium fluoride substrates (Rubicon Technology, Inc.). Spin-cast films were characterized with variable angle spectroscopic ellipsometry (V-VASE, J. A. Woollam Corp.) as isotropic materials for the determination of refractive index and thickness.

Photodimerization of Polymer Films. Irradiation of **Polymer** films was performed at both 25 and 120 °C under argon with a 500 W Hg−Xe lamp (model 66142, Oriel) equipped with a filter (model 87031, Oriel) that cuts off wavelengths below 300 nm. Linear polarization was accomplished using a polarizing beam splitter (HPB-308 nm, Lambda Research Optics, Inc). The irradiation intensity was monitored by a UVX digital radiometer coupled with a UVX-31 sensor (UVP, Inc.). The insolubility of irradiated films was ascertained by UV−vis absorption spectroscopy after soaking in chloroform for 2 min.

Photoalignment of a Nematic Liquid Crystal and Glassy−Nematic Oligofluorenes. For the characterization of the ability to orient a nematic liquid crystal, the irradiated **Polymer** films on fused silica substrates were used to prepare 10-μm-thick sandwiched cells. A commercially available nematic liquid crystal, E7 (Merck), containing a probing dichroic dye, M-137 (Mitsui Toatsu Dyes, Ltd.), at 0.3 wt % was injected into the cell gap in the isotropic state (at 65 °C) to avoid flow-induced alignment. After thermal annealing at 55 °C for 0.5 h, the cells were cooled at 10 °C/h to room temperature. A UV−vis−NIR spectrophotometer (Lambda-900, Perkin-Elmer) equipped with a linear polarizer (HNP′B, Polaroid) was used to measure the orientational order parameter. Fresnel reflections from the air−glass interfaces were accounted for using a reference cell comprising an index-matching fluid between two alignment-treated substrates. The **Polymer** film's ability to orient monodisperse glassy−nematic oligofluorenes was also appraised. Approximately 50-nm-thick oligofluorene films were spin-cast on photoalignment films from 0.5 wt % chloroform solutions. After vacuum-drying overnight, the oligofluorene films were thermally annealed above their glass transition temperatures for 0.5 h under argon followed by cooling to room temperature. Polarized UV−vis absorption spectroscopy was employed to determine the orientational order parameter.

Results and Discussion

Depicted in Chart 1 are the molecular structures of coumarin **Monomer** and **Dimer** as well as the coumarin-containing **Polymer** and **Copolymer** with their glass transition temperatures and average molecular weights. The regioisomerism of **Dimer**, *syn-hh*, was positively identified by proton NMR signals attributable to the cyclobutane ring[50] (see Figures S.1 and S.2 in the Supporting Information). The issue of photodegradation was addressed using the FTIR spectroscopic technique. **Monomer** and **Dimer** were doped in **PMMA** [poly(methyl methacrylate), Polysciences, Inc., $\bar{M}_w = 75\,000$ g/mol], at $Y = 0.154$, the mole fraction of coumarin moieties on the basis of methyl

Table 1. FTIR Peak Assignment for Polymer, Monomer, Dimer, and PMMA Used in the Present Study[a–c]

peak ID	wavenumber, cm^{-1} Polymer	Monomer	Dimer	PMMA	assignment
i	1770	–	1776	–	C=O stretching (*syn-hh* dimer)
ii	1734	1731	1731	1729	C=O stretching (monomer)
iii	1605	1605	1603	–	ring C=C stretching
iv	1511	1511	1511	–	ring C=C stretching
v	1249	1248	1241	1241	C–C–O ester stretching
vi	1170	1168	1168	–	C(C=O)–O sym stretching
vii	1149	1148	1148	1148	unconjugated ester stretching
viii	1122	1122	1115	–	C(C=O)–O sym stretching

[a] Li, W.; Thompson, H.; Fox, M. A. *J. Am. Chem. Soc.* **1997**, *119*, 7211–7217. [b] Obi, M.; Morino, S.; Ichimura, K. *Chem. Mater.* **1999**, *11*, 656–664. [c] Jackson, P. O.; O'Neill, M.; Duffy, W. L.; Hindmarsh, P.; Kelly, S. M.; Owen, G. J. *Chem. Mater.* **2001**, *13*, 694–703.

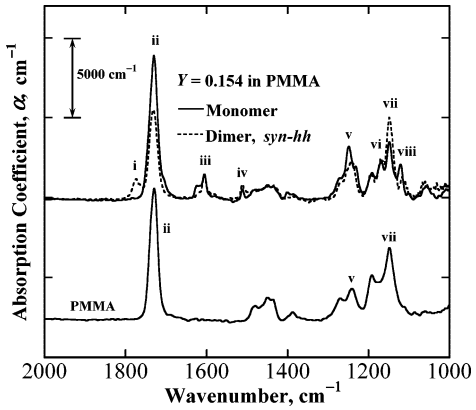

Figure 1. FTIR spectra of an undoped **PMMA** film in addition to **PMMA** films doped with **Monomer** and **Dimer** at $Y = 0.154$ to ensure miscibility, all approximately 100 nm in thickness; assignment of peaks i–viii made in Table 1.

methacrylate units. Shown in Figure 1 are the FTIR spectra of approximately 100-nm-thick spin-cast films of **PMMA** doped with **Monomer** and **Dimer** as well as that of a **PMMA** film with peaks i–viii assigned in Table 1.

For the calculation of the absorption coefficient, α, i.e. absorbance per unit thickness, the film thickness was determined by spectroscopic ellipsometry. A comparison of the three spectra led to the conclusion that photodimerization resulted in the growth of peaks i and vii, the depletion of peaks ii, iii, v, and viii, but little or no change in peaks iv and vi. The FTIR spectra of 25-nm-thick **Polymer** films irradiated at 25 °C up to a fluence up to 10 J/cm^2 are compiled in Figure 2. The changes in intensities of all the peaks are consistent with the difference between **Monomer** and **Dimer** as identified in Figure 2. Furthermore, in the 3000–3600 cm^{-1} spectral range, no O–H or COO–H stretching bands are visible, suggesting the absence of photooxidation. Therefore, the FTIR spectroscopic analysis has provided convincing evidence that the **Polymer** films are stable against photodegradation. The same conclusion was reached with **Polymer** films irradiated at 120 °C (see Figures S.3 and S.4 in the Supporting Information). Additional evidence of photostability will be furnished below with UV–vis absorption spectroscopy.

To establish UV–vis absorption spectroscopy as a technique for determining the extent of photodimerization of coumarin, *X*, **Monomer** and **Dimer** were doped into **PMMA** at $Y = 0.050$ for the preparation of approximately 100-nm-thick films via spin casting. The UV–vis absorption spectra shown in Figure 3 indicate that **Dimer** is transparent in the spectral region above 300 nm, which not only ensures that coumarin monomers in **Polymer** be the sole recipient of polarized UV-irradiation but

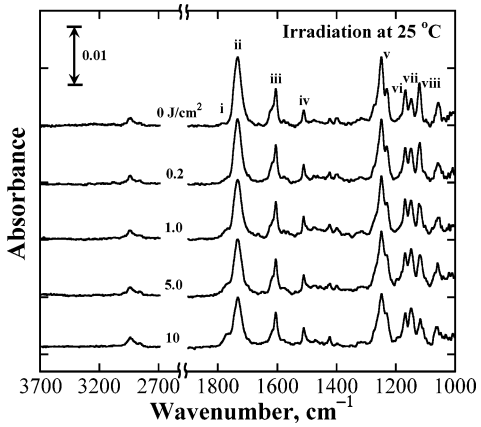

Figure 2. FTIR spectra of 25-nm-thick **Polymer** films exposed to linearly polarized UV-irradiation to a varying fluence at 25 °C; peaks i–viii as assigned in Table 1 for comparison to those identified in Figure 1, showing absence of degradation.

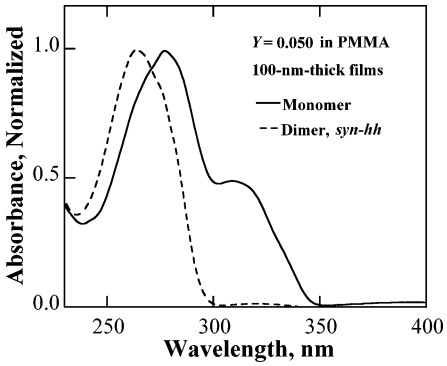

Figure 3. Normalized UV–vis absorption spectra of approximately 100-nm-thick films consisting of **Monomer** and **Dimer** doped at Y = 0.050 in **PMMA** films.

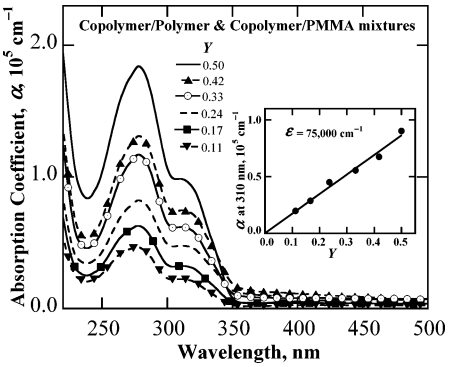

Figure 4. UV–vis absorption spectra of approximately 80-nm-thick films of films comprising **Copolymer**/**Polymer** and **Copolymer**/**PMMA** mixtures to evaluate absorption coefficient as a function of coumarin mole fraction, *Y*; the direct proportionality between α and *Y* shown in the inset yielded an extinction coefficient $\epsilon = 75\,000$ cm^{-1}.

also enables *X* to be quantified by monitoring the monomer absorbance at 310 nm.

A series of **Copolymer/Polymer** and **Copolymer/PMMA** mixtures were prepared for the determination of α as a function of *Y*. The results are presented in Figure 4, including the direct proportionality of α (at 310 nm) to *Y* displayed in the inset for the determination of *X* by monitoring the decreasing absorbance of coumarin monomer with irradiation time. Through spin coating from dilute chloroform solutions, **Polymer** was prepared into 10-nm-thick films for irradiation with a linearly polarized UV-source above 300 nm to a varying fluence. Although the resultant dimer's regioisomerism in the irradiated films is

Chart 2. Molecular Structures of Monodisperse Oligofluorenes Reported Previously[51] and Tested in This Study for Photoalignment[a]

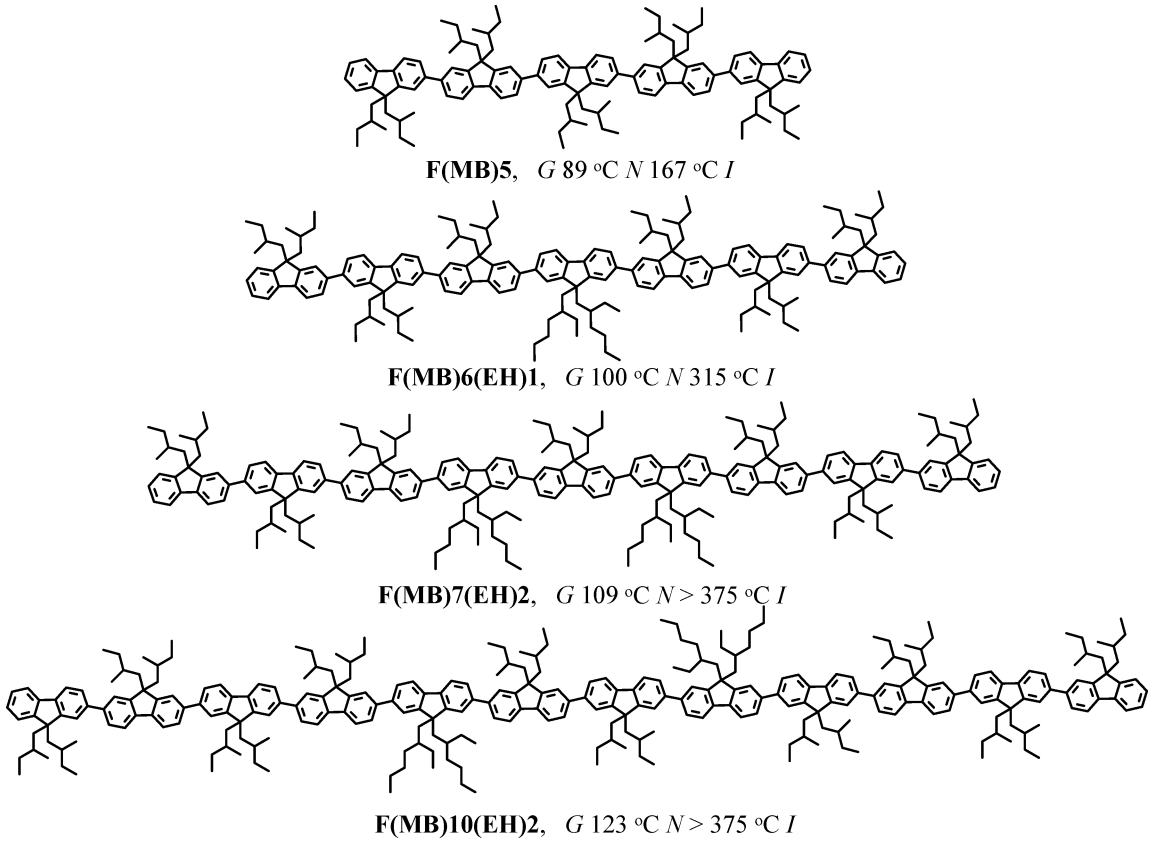

F(MB)5, *G* 89 °C *N* 167 °C *I*

F(MB)6(EH)1, *G* 100 °C *N* 315 °C *I*

F(MB)7(EH)2, *G* 109 °C *N* > 375 °C *I*

F(MB)10(EH)2, *G* 123 °C *N* > 375 °C *I*

[a] Symbols: G, glassy; N, nematic; I, isotropic.

Table 2. Extent of Dimerization, *X*, and Liquid Crystal Orientational Order Parameter, S_{lc}, as Functions of Fluence at Different Irradiation Temperatures[a]

fluence, J/cm^2	25 °C[b]		120 °C[c]	
	X	S_{lc}	*X*	S_{lc}
0.1	0.12	−	0.18	−
0.2	0.18	−	0.24	∥ 0.73
0.5	0.27	−	0.35	∥ 0.75
1.0	0.29	∥ 0.77	0.45	∥ 0.71
2.0	0.38	∥ 0.75	0.53	−
3.0	0.42	∥ 0.74	−	∥ 0.75
4.0	0.46	⊥ 0.76	0.57	∥ 0.73
5.0	0.48	⊥ 0.73	0.59	⊥ 0.80
10	0.48	⊥ 0.75	0.59	⊥ 0.75

[a] Presented values for *X* and S_{lc} both accompanied by an uncertainty ± 0.02; symbols ∥ and ⊥ in front of S_{lc} represent a nematic director parallel and perpendicular to the polarization axis, respectively. [b] Insolubility of 10-nm-thick film achieved at 1 J/cm^2. [c] Insolubility of 10-nm-thick film achieved at 0.2 J/cm^2.

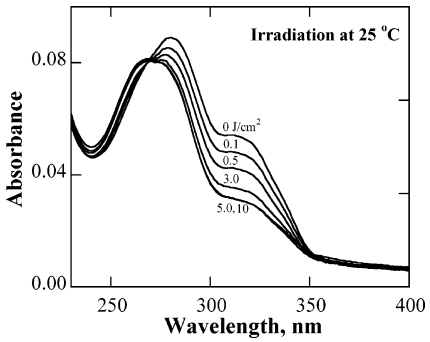

Figure 5. UV−vis absorption spectra of 10-nm-thick **Polymer** films exposed to linearly polarized UV-irradiation to a varying fluence at 25 °C; absence of degradation is evidenced by the presence of an isobestic point.

unknown, these films' UV−vis absorption spectra are not expected to undergo a major spectral shift from that of the model **Dimer** with a *syn-hh* regioisomerism.[50] The UV−vis absorption spectra of 25-nm-thick **Polymer** films irradiated at 25 °C are compiled in Figure 5 for the calculation of *X* using coumarin monomer's absorbance at 310 nm. The presence of an isobestic point is an indication of stability against photodegradation up to 10 J/cm^2. A similar set of spectra was acquired for irradiation at 120 °C (see Figure S.5 in the Supporting Information).

The ability of the UV-irradiated films to orient liquid crystals was appraised using nematic liquid crystal fluid cells. A dichroic dye, M-137, was employed to track the nematic director of a commercially available liquid crystal fluid, E7, on the grounds that the dye molecule's transition dipole is parallel to the liquid crystal's long molecular axis, as demonstrated by liquid crystal orientation on uniaxially rubbed polyimide films. With 0.3 wt % of M-137 in E7, 10-μm-thick liquid crystal cells were prepared between fused silica substrates, both coated with photoalignment films that had been irradiated to varying fluences. The UV−vis absorption dichroism at 643 nm served to determine the liquid crystal's orientational order parameter, $S_{lc} = (R - 1)/(R + 2)$, in which the dichroic ratio *R* represents the absorbance parallel over that perpendicular to the dye molecule's absorption dipole. The calculated S_{lc} values are prefixed by ∥ and ⊥ for the parallel and perpendicular orientations, respectively, of the nematic director to the polarization axis of irradiation. The oft-quoted transition from parallel to perpendicular orientation of an overlaying nematic liquid crystal is qualitatively understood under the premise that a small fraction of oriented liquid crystal molecules will motivate the rest to follow. At a low fluence of linearly polarized irradiation of the photoalignment film, dimerization is limited to coumarin moieties whose absorption dipoles fall along the polarization

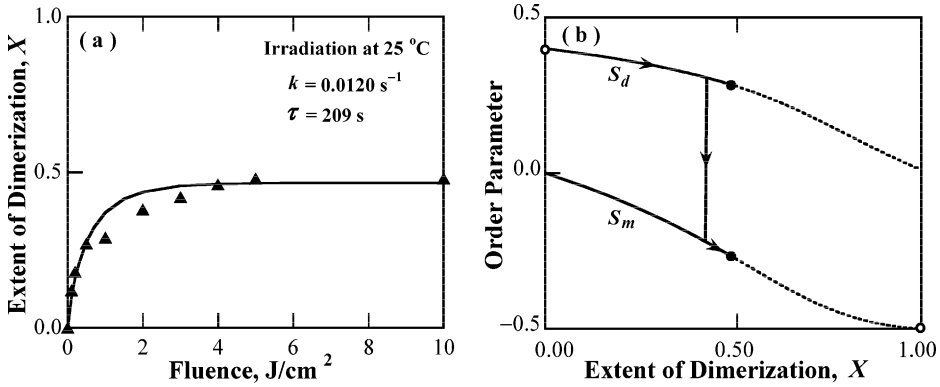

Figure 6. Kinetic modeling of a 10-nm-thick **Polymer** film exposed to linearly polarized UV-irradiation at 25 °C: (a) extent of dimerization, X, as a function of fluence, where experimental data shown to be well represented by model with the specified k and τ values and (b) orientational order parameter, S_d and S_m, calculated for the **Polymer** film as functions of X; symbols: open circles for discontinuity, and filled circles for terminal photodimerization at $X = 0.48$; transition from a parallel to a perpendicular liquid crystal orientation observed at $X = 0.44$.

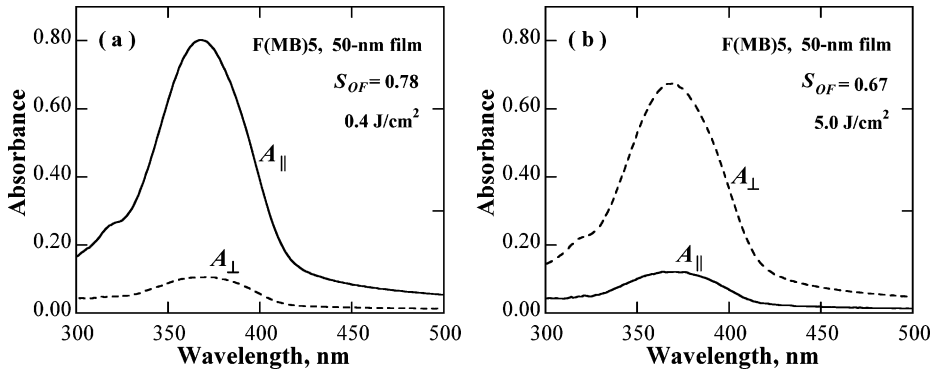

Figure 7. UV−vis absorption dichroism of 50-nm-thick a pentafluorene film on 10-nm-thick **Polymer** film irradiated at 120 °C to (a) 0.4 J/cm^2 and (b) 5.0 J/cm^2; $A_{\parallel}$ and $A_{\perp}$ represent absorbance parallel and perpendicular, respectively to the polarization axis of UV-irradiation.

Table 3. Orientational Order Parameter, S_{OF}, for Oligofluorenes[a] on Polymer Photoalignment Film[b]

	F(MB)5	F(MB)6(EH)1	F(MB)7(EH)2	F(MB)10(EH)2
T_g, °C	89	100	109	123
T_{anneal},[c] °C	120	130	140	145
S_{OF}	0.76 ± 0.02	0.75 ± 0.02	0.72 ± 0.01	0.68 ± 0.01

[a] Synthesis and characterization of oligofluorenes reported in *Chem. Mater.* **2003**, *15*, 542−549; 50-nm-thick films annealed for 30 min under argon. [b] 10-nm-thick film irradiated with 0.4 J/cm^2 at 120 °C under argon. [c] Annealing temperature.

axis. These preferentially placed coumarin dimers manage to orient the nematic liquid crystal along the polarization axis of UV-irradiation. At a high fluence, unreacted coumarin moieties have their absorption dipoles lying largely perpendicular to the polarization axis, while coumarin dimers are nearly randomly placed. Thus, for a given photoalignment film, there exists a critical fluence at which crossover in liquid crystal orientation takes place.

Table 2 summarizes X and S_{lc} as functions of fluence for irradiation at 25 and 120 °C, two representative temperatures across $T_g = 68$ °C in a pristine **Polymer** film. Regardless of the irradiation temperature, X reached an asymptotic value because of the drastically diminished mobility of coumarin moieties and, consequently, the vanishing reaction rate at an advanced stage of dimerization. Compared to 25 °C, irradiation at 120 °C resulted in a higher asymptotic conversion, $X = 0.59$ versus 0.48, as well as a delayed crossover in liquid crystal orientation, $X = 0.58$ versus 0.44. Both observations can be understood on the basis of the higher mobility of coumarin moieties at 120 °C, including rotational diffusion favorable to dimerization. Rotational diffusion resulted in the formation of more dimeric coumarins along the polarization axis of irradiation at the expense of monomeric coumarins, thus sustaining the parallel liquid crystal orientation toward a higher monomer conversion. In any event, the extent of coumarin dimerization, instead of photodegradation,[39] is responsible for the observed crossover behavior.

In the qualitative picture depicted above, it is evident that X is the ultimate parameter affecting the crossover behavior. In a recent paper,[49] we have constructed a kinetic model for the description of X as a function of irradiation time, t

$$X(t) = \frac{\int_0^{\pi} X_d(\theta,t) \sin\theta \, d\theta}{\int_0^{\pi} \sin\theta \, d\theta} = 1 - \sqrt{\frac{\pi}{4A(t)}} \, \mathrm{erf}[\sqrt{A(t)}] \qquad (1)$$

in which θ is the angle between monomeric coumarin's absorption dipole and the polarization axis of UV-irradiation, and $A(t) = k\tau[1 - \exp(-t/\tau)]$ with k and τ denoting, respectively, the rate constant and the time constant characteristic of the exponentially decaying dimerization rate. The kinetic model was further employed to describe the temporal evolution of the orientational order parameters,[49] S_d and S_m, characterizing the reacted and unreacted coumarin moieties, respectively:

$$S_d(t) = \frac{[3 - 2A(t)]\sqrt{\pi}\mathrm{erf}[\sqrt{A(t)}] - 6\sqrt{A(t)}\exp[-A(t)]}{4A(t)\{\sqrt{\pi}\mathrm{erf}[\sqrt{A(t)}] - 2\sqrt{A(t)}\}} \qquad (2)$$

$$S_m(t) = \frac{3}{4A(t)} - \frac{1}{2} - \frac{3\exp[-A(t)]}{2\sqrt{\pi A(t)}\,\mathrm{erf}[\sqrt{A(t)}]} \qquad (3)$$

As the mobility of the reacted and unreacted coumarin moieties in the dimerization process was not accounted for, we

will restrict our quantitative interpretation to results from irradiation at 25 °C, viz. below T_g = 68 °C, as the more appropriate system for testing the model. It is recognized, however, that the orientations of reacted and unreacted coumarin moieties are subject to thermal relaxation, depending on temperature and the extent of dimerization. The experimental data for X are presented in Figure 6a as a function of fluence at a constant irradiation power of 4.8 mW/cm^2. A reasonably good fit to eq 1 emerged with $k = 0.0120$ s^{-1} and $\tau = 209$ s, which were then entered into eqs 2 and 3 to calculate S_d and S_m as functions of X. The profiles shown in Figure 6b serve to assess the relative importance of three parameters affecting liquid crystal orientation on the photoalignment film: relative abundance of the reacted and unreacted coumarin moieties, their orientational order parameters, and the energetics of their interactions with liquid crystal molecules. At the crossover point of $X = 0.44$, the reacted and unreacted coumarin moieties are present at a mole fraction of 0.44 and 0.56, respectively, with $S_d = 0.30$ and $|S_m| = 0.23$. In the light of these two counteracting factors, one plausible conclusion is that liquid crystal molecules interact more favorably with monomeric coumarin pendants than the dimeric counterparts.

In addition to the nematic liquid crystal fluid, the amenability of glassy−nematic oligofluorenes to photoalignment was also tested using 10-nm-thick **Polymer** films irradiated with 0.4 J/cm^2 at 120 °C. Together with their glass and nematic-to-isotropic transition temperatures, the molecular structures of select oligofluorenes are depicted in Chart 2.[51] Approximately 50-nm-thick films of oligofluorenes were spin-cast on 10-nm-thick photoalignment films for thermal annealing above oligofluorenes' respective T_g values for 0.5 h under argon with subsequent cooling to room temperature to arrive at uniaxially oriented glassy−nematic films. The orientational order parameter, S_{OF}, of these single-substrate films was characterized by UV−vis absorption dichroism to be parallel to the polarization axis.

The data presented in Table 3 reveal a decreasing S_{OF} value with an increasing oligofluorene chain length, which is contrary to the prior observation on rubbed polyimide alignment films under similar annealing conditions.[51]

Nevertheless, the S_{OF} value of 0.76 achieved with **F(MB)5** (a pentafluorene) is comparable to that on a rubbed polyimide film. The decreasing S_{OF} value with an increasing oligofluorene chain length on the photoalignment film could have arisen from the required annealing temperature that increases with chain length, causing the relaxation of orientation on the part of dimerized coumarin moieties. Molecular relaxation is expected to take place at temperatures both above T_g and, to a lesser extent, below T_g. Photodimerization of coumarin moieties may elevate T_g to a certain degree above the pristine **Polymer** film. Therefore, a highly cross-linked (i.e. dimerized) photoalignment film with an elevated T_g is desirable for practical applications that entail thermal annealing of the overlaying films. As illustrated with **F(MB)5** in Figure 7, the glassy−nematic film underwent a transition from a parallel to a perpendicular orientation on the underlying photoalignment film that had been irradiated with 0.4 and 5.0 J/cm^2 both at 120 °C. This behavior is similar to that of nematic liquid crystal fluid films contained between a pair of substrates coated with photoalignment films.

Conclusions

To examine the orientation of a nematic liquid crystal, alignment films comprising a polymethacrylate backbone carrying 7-benzoyloxycoumarin pendants with a T_g of 68 °C was treated with linearly polarized UV-irradiation to varying fluences at 25 and 120 °C. Model **Monomer** and **Dimer** as well as **Copolymer** were also synthesized and characterized not only to permit an investigation of photodegradation but also to establish the extent of photodimerization, X, in **Polymer** films for elucidating liquid crystal orientation. The ability of the UV-irradiated **Polymer** film to orient monodisperse glassy−nematic oligofluorenes was also demonstrated. Key observations are summarized as follows:

(1) The UV−vis and FTIR spectroscopic analyses revealed the photostability of **Polymer** films upon UV-irradiation at 25 and 120 °C up to 10 J/cm^2. An advanced stage of dimerization, as opposed to photodegradation, was found to be responsible for the observed crossover from a parallel to a perpendicular liquid crystal orientation with reference to the polarization axis of irradiation.

(2) In comparison to 25 °C, irradiation at 120 °C resulted in a higher asymptotic dimerization, $X = 0.59$ versus 0.48, and a delayed crossover in liquid crystal orientation, $X = 0.58$ versus 0.44. Both findings are attributable to the thermally activated rotational diffusion of monomeric coumarin pendants during photodimerization.

(3) The crossover behavior in liquid crystal orientation for UV-irradiation at 25 °C was interpreted with a kinetic model, leading to the conclusion that liquid crystal molecules interact more favorably with coumarin monomers than with dimers in view of the opposing effects of relative abundance and orientational order on the parts of the two motivating species.

(4) Through thermal annealing above their T_g values with subsequent cooling to room temperature, glassy−nematic oligofluorene films were shown to orient on UV-irradiated **Polymer** films. In the case of pentafluorene, the orientational order parameter was comparable to that achieved on a rubbed polyimide film. Moreover, the pentafluorene film was found to undergo a transition from a parallel (at 0.4 J/cm^2) to a perpendicular (at 5.0 J/cm^2) orientation on **Polymer** films irradiated at 120 °C. The orientational order parameter, however, was found to decrease with an increase in the oligofluorene's chain length, presumably because of the increased annealing temperature that causes an orientational relaxation on the part of the dimerized coumarin moieties.

Acknowledgment. The authors thank Jason U. Wallace of the Department of Chemical Engineering, University of Rochester for technical advice and helpful discussions. They are also grateful for the financial support provided by the Eastman Kodak Co., the New York State Center for Electronic Imaging Systems, and the National Science Foundation under Grant CTS-0204827. Additional funding was provided by the Department of Energy Office of Inertial Confinement Fusion under Cooperative Agreement No. DE-FC03-92SF19460 with the Laboratory for Laser Energetics and the New York State Energy Research and Development Authority. The support of DOE does not constitute an endorsement by DOE of the views expressed in this article.

Supporting Information Available: Reaction schemes and procedures for material synthesis and purification of **Monomer**, **Dimer**, **Polymer**, and **Copolymer**; **Dimer**'s regioisomerism by ^{1}H NMR spectral analysis; and FTIR and UV−vis spectra of **Polymer** films irradiated at 120 °C. This material is available free of charge via the Internet at http://pubs.acs.org.

References and Notes

(1) Grell, M.; Bradley, D. D. C.; Inbasekaran, M.; Woo, E. P. *Adv. Mater.* **1997**, *9*, 798−802.

(2) Whitehead, K. S.; Grell, M.; Bradley, D. D. C.; Jandtke, M.; Strohriegl, P. *Appl. Phys. Lett.* **2000**, *76*, 2946−2948.
(3) Grell, M.; Knoll, W.; Lupo, D.; Meisel, A.; Miteva, T.; Neher, D.; Nothofer, H.-G.; Scherf, U.; Yasuda, A. *Adv. Mater.* **1999**, *11*, 671−675.
(4) Chen, A. C. A.; Culligan, S. W.; Geng, Y.; Chen, S. H.; Klubek, K. P.; Vaeth, K. M.; Tang, C. W. *Adv.* Mater. **2004**, *16*, 783−788.
(5) Culligan, S. W.; Geng, Y.; Chen, S. H.; Klubek, K.; Vaeth, K. M.; Tang, C. W. *Adv. Mater.* **2003**, *15*, 1176−1180.
(6) Geng, Y.; Chen, A. C. A.; Ou, J. J.; Chen, S. H.; Klubek, K.; Vaeth, K. M.; Tang, C. W. *Chem. Mater.* **2003**, *15*, 4352−4360.
(7) van Breemen, A. J. J. M.; Herwig, P. T.; Ceciel, H. T. C.; Sweelssen, J.; Schoo, H. F. M.; Setayesh, S.; Hardeman, W. M.; Martin, C. A.; de Leeuw, D. M.; Valeton, J. J. P.; Bastiaansen, C. W. M.; Broer, D. J.; Popa-Merticaru, A. R.; Meskers, S. C. J. *J. Am. Chem. Soc.* **2006**, *128*, 2336−2345.
(8) Sirringhaus, H.; Wilson, R. J.; Friend, R. H.; Inbasekaran, M.; Wu, W.; Woo, E. P.; Grell, M.; Bradley, D. D. C. *Appl. Phys. Lett.* **2000**, *77*, 406−408.
(9) Chen, L.-Y.; Hung, W.-Y.; Lin, Y.-T.; Wu, C.-C.; Chao, T.-C.; Hung, T.-H.; Wong, K.-T. *Appl. Phys. Lett.* **2005**, *87*, 112103/1−112103/3.
(10) Yasuda, T.; Fujita, K.; Tsutsui, T.; Geng, Y.; Culligan, S. W.; Chen, S. H. *Chem. Mater.* **2005**, 17, 264−268.
(11) Ishihara, S. *IEEE/OSA J. Display Technol.* **2005**, *1*, 30−40.
(12) Bechtold, I. H.; De Santo, M. P.; Bonvent, J. J.; Oliveira, E. A.; Barberi, R.; Rasing, Th. *Liq. Cryst.* **2003**, *30*, 591−598.
(13) Schadt, M.; Seiberle H.; Schuster, A. *Nature (London)* **1996**, *381*, 212−215.
(14) Gupta, V. K.; Abbott, N. L. *Science* **1997**, *276*, 1533−1536.
(15) Patel, J. J.; Rastani, K. *Opt. Lett.* **1991**, *16*, 532−534.
(16) Chen. J.; Bos, P. J.; Vithana, H.; Johnson, D. L. *Appl. Phys. Lett.* **1995**, *67*, 2588−2590.
(17) Hasegawa, M.; Taira, Y. *J. Photopolym. Sci. Technol.* **1995**, *8*, 241−248.
(18) Gong, S.; Kanicki, J.; Ma, L.; Zhong, J. Z. Z. *Jpn. J. Appl. Phys.* **1999**, *38*, 5996−6004.
(19) Lu, J.; Deshpande, S. V.; Gulari, E.; Kanicki, J.; Warren, W. L. *J. Appl. Phys.* **1996**, *80*, 5028−5034.
(20) Sung, S.-J.; Lee, J.-W.; Kim, H.-T.; Park, J.-K. *Liq. Cryst.* **2002**, *29*, 243−250.
(21) (a) Xu, C.; Shiono, T.; Ikeda, T.; Wang, Y.; Takeuchi, Y. *J. Mater. Chem.* **2003**, *13*, 669−671. (b) Zhong, Z.-X.; Li, X.; Lee, S. H.; Lee, M.-H. *Appl. Phys. Lett.* **2004**, *85*, 2520−2522.
(22) Gibbons, W. M.; Shannon, P. J.; Sun, S.-T.; Swetlin, B. J. *Nature* **1991**, 351, 49−50.
(23) Shannon, P. J.; Gibbons, W. M.; Sun, S.-T. *Nature (London)* **1994**, *368*, 532−533.
(24) Ichimura, K.; Suzuki, Y.; Seki, T.; Hosoki, A.; Aoki, K. *Langmuir* **1988**, *4*, 1214−1216.
(25) Ichimura, K. *Chem. Rev.* **2000**, *100*, 1847−1874.
(26) Ikeda, T. *J. Mater. Chem.* **2003**, *13*, 2037−2057.
(27) Furumi, S.; Kidowaki, M.; Ogawa, M.; Nishimura, Y.; Ichimura, K. *J. Phys. Chem. B* **2005**, *109*, 9245−9254.
(28) Sévigny, S.; Bouchard, L.; Montallebi, S.; Zhao, Y. *Liq. Cryst.* **2005**, *32*, 599−607.
(29) Schadt, M.; Schmitt, K.; Kozinkov, V.; Chigrinov, V. *Jpn. J. Appl. Phys.* **1992**, *31*, 2155−2164.
(30) Schadt, M.; Seiberle, H.; Schuster, A.; Kelly, S. M. *Jpn. J. Appl. Phys.* **1995**, *34*, L764-L767.
(31) Cull, B.; Shi, Y.; Kumar, S.; Schadt, M. *Phys. Rev. E.* **1996**, *53*, 3777−3781.
(32) Obi, M.; Morino, S.; Ichimura, K. *Jpn. J. Appl. Phys.* **1999**, *38*, L145−L147.
(33) Kawatsuki, N.; Ono, H.; Takatsuka, H.; Yamamoto, T.; Sangen, O. *Macromolecules* **1997**, *30*, 6680−6682.
(34) (a) Kawatsuki, N.; Matsuyoshi, K.; Hayashi, M.; Takatsuka, H.; Yamamoto, T. *Chem. Mater.* **2000**, *12*, 1549−1555. (b) Kawatsuki, N.; Takatsuka, H.; Yamamoto, T.; Ono, H. *Jpn. J. Appl. Phys.* **1997**, *36*, 6464−6469.
(35) Ichimura, K.; Akita, Y.; Akiyama, H.; Kudo, K.; Hayashi, Y. *Macromolecules* **1997**, *30*, 903−911.
(36) Stump, A.; Gubler, U.; Bosshard, C. *Opt. Lett.* **2005**, *30*, 1333−1335.
(37) Perny, S.; Barny, P. L.; Delaire, J.; Buffeteau, T.; Sourisseau, C.; Dozov, I.; Forget, S.; Martinot-Lagarde, P. *Liq. Cryst.* **2000**, *27*, 329−340.
(38) Obi, M.; Morino, S.; Ichimura, K. *Chem. Mater.* **1999**, *11*, 656−664.
(39) Jackson, P. O.; O'Neill, M.; Duffy, W. L.; Hindmarsh, P.; Kelly, S. M.; Owen, G. J. *Chem. Mater.* **2001**, *13*, 694−703.
(40) Kawatsuki, N.; Goto, K.; Yamamoto, T. *Liq. Cryst.* **2001**, *28*, 1171−1176.
(41) Lee, J.; Lee, J.-I.; Sung, S.-J.; Chu, H. Y.; Park, J.-K.; Shim, H.-K. *Macromol. Chem. Phys.* **2004**, *205*, 2245−2251.
(42) Tian, Y.; Akiyama, E.; Nagase, Y. *J. Mater. Chem.* **2003**, *13*, 1253−1258.
(43) Huang, D. D.; Kozenkov, V.; Chigrinov, V.; Kwok, H. S.; Takada, H.; Takatsu, H. *Jpn. J. Appl. Phys.* **2005**, *44*, 5117−5118.
(44) Contoret, A. E. A.; Farrar, S. R.; Jackson, P. O.; Khan, S. M.; May, L.; O'Neill, M.; Nicholls, J. E.; Kelly, S. M.; Richards, G. J. *Adv. Mater.* **2000**, *12*, 971−974.
(45) Aldred, M. P.; Contoret, A. E. A.; Farrar, S. R.; Kelly, S. M.; Mathieson, D.; O'Neill, M. O.; Tsoi, W. C.; Vlachos, P. *Adv. Mater.* **2005**, *17*, 1368−1372.
(46) Sainova, D.; Zen, A.; Nothofer, H.-G.; Asawapirom, U.; Scherf, U.; Hagen, R.; Bieringer, T.; Kostromine, S.; Neher, D. *Adv. Funct. Mater.* **2002**, *12*, 49−57.
(47) Jin, S.-H.; Seo, H.-U.; Nam, D.-H.; Shin, W. S.; Choi, J.-H.; Yoon, U. C.; Lee, J.-W.; Song, J.-G.; Shin, D.-M.; Gal, Y.-S. *J. Mater. Chem.* **2005**, *15*, 5029−5036.
(48) Chou, W.-Y.; Cheng, H.-L. *Adv. Funct. Mater.* **2004**, *14*, 811−815.
(49) Kim, C.; Trajkovska, A.; Wallace, J. U.; Chen, S. H. *Macromolecules* **2006**, *39*, 3817−3823.
(50) Yu, X.; Scheller, D.; Rademacher, O.; Wolff, T. *J. Org. Chem.* **2003**, *68*, 7386-7399.
(51) Geng, Y.; Culligan, S. W.; Trajkovska, A.; Wallace, J. U.; Chen, S. H. *Chem. Mater.* **2003**, *15*, 542−549.

MA060959S